ARTICLE

OPEN

Check for updates

The unitary dependence theory for characterizing quantum circuits and states

Zixuan Hu [1] & Sabre Kais [1✉]

Most existing quantum algorithms are discovered accidentally or adapted from classical algorithms, and there is the need for a systematic theory to understand and design quantum circuits. Here we develop a unitary dependence theory to characterize the behaviors of quantum circuits and states in terms of how quantum gates manipulate qubits and determine their measurement probabilities. Compared to the conventional entanglement description of quantum circuits and states, the unitary dependence picture offers more practical information on the measurement and manipulation of qubits, easier generalization to many-qubit systems, and better robustness upon partitioning of the system. The unitary dependence theory can be applied to systematically understand existing quantum circuits and design new quantum algorithms.

[1] Department of Chemistry, Department of Physics, and Purdue Quantum Science and Engineering Institute, Purdue University, West Lafayette, IN 47907, USA. ✉email: kais@purdue.edu

Over several decades, the search for quantum algorithms with efficient quantum circuit implementations has resulted in numerous theoretical and technological advancements[1–14]. Notable quantum algorithms with the potential to outperform classical algorithms include: the phase estimation algorithm[15], Shor's factorization algorithm[16], the Harrow-Hassidim-Lloyd algorithm for linear systems[17], the hybrid classical-quantum algorithms[18,19], the quantum machine learning algorithms[20–22], and quantum algorithms for open quantum dynamics[23–25]. Despite the expansive selection of ideas, most existing quantum algorithms are either discovered accidentally or adapted from classical algorithms, and a systematic way to understand and design quantum algorithms with efficient quantum circuit implementation is currently lacking. Considering the enormous search space of quantum circuits, we need a general theory to classify all quantum circuits and states, and then study their behaviors based on the classification. To this end, we have previously proposed a theory to classify all quantum circuits of a given length into finite types based on the "qubit functional configuration"[26].

In this work we develop a "unitary dependence theory" to characterize the behaviors of quantum circuits and states in terms of how quantum gates manipulate qubits and determine their measurement probabilities. Any quantum circuit can be decomposed into a sequence of elementary gates that include 1-qubit unitaries and 2-qubit CNOT gates. The initial state is transformed by the circuit into the final state which then undergoes projection measurements in the computational basis $\{|0\rangle, |1\rangle\}$. The probability of measuring $|0\rangle$ versus $|1\rangle$ on each qubit then determines the measurement statistics of the final state which can be used to characterize the behavior of the quantum circuit and the final state. In this work we study how the probabilities of measuring each qubit are affected by elementary gates. The basic rules are: 1. a 1-qubit unitary U_k makes the target qubit q_k's measurement probabilities depend on U_k; 2. a CNOT gate $CX_{j\to k}$ copies all the control qubit q_j's dependences to the target qubit q_k. By these rules, each qubit q_k at the final state has its own collection of dependences that may be created on itself by some U_k or copied to it from other qubits by some CNOT gates. While a dependence may be copied from other qubits, it must have been created by some U_i on another qubit q_i – i.e., any given dependence can be traced back to the original 1-qubit unitary that has created it in the first place – therefore a complete unitary dependence picture of which qubit depends on which 1-qubit unitaries can be drawn by analyzing the gate sequence of a quantum circuit. The dependence picture carries important information that helps us understand the behaviors of quantum circuits. For example, if two qubits share dependences on some 1-qubit unitaries, then their measurement probabilities must be dependent; while if they do not share any dependence, their measurement probabilities must be independent. From the circuit design perspective, varying the parameters of a 1-qubit unitary shared by multiple qubits allows us to manipulate the measurement probabilities of all involved qubits together; while qubit-specific manipulations have to be implemented with 1-qubit unitaries that are unique to the particular qubit. The dependence picture is a new perspective for characterizing quantum circuits and states because it is distinct from the conventional way of using entanglement as a descriptor of complexity[27]. Compared to the abstract formalism of multi-qubit entanglement[28–30], the dependence picture offers more practical information on the measurement and manipulation of qubits, easier generalization to many-qubit systems, and better robustness upon partitioning of the system. Furthermore, in a deeper discussion of the unitary dependence theory, we find that under certain conditions the dependences originated from the same unitary source can cancel when duplicated on the same

qubit, which reduces complexity and simplifies the dependence picture. Interestingly, in studying the cancellability of dependences, we find that entanglement can protect the cancellability from getting broken by local 1-qubit unitaries, and thus an intricate relation between the unitary dependence and entanglement exists. Finally the theory has been applied to the widely-used hardware-efficient ansatz[31–34] to demonstrate its ability to characterize the behaviors of different ansatzes in variational quantum algorithms.

In summary, we propose a unitary dependence theory to characterize quantum circuits and states in terms of how quantum gates manipulate qubits and determine their measurement probabilities. A complete unitary dependence picture can be generated by analyzing the gate sequence of a quantum circuit. The theory has several advantages over the conventional entanglement description of quantum circuits and states, and can be applied to systematically understand existing quantum circuits and design new quantum algorithms.

Results and discussion
Basic rules for the creation and copying of unitary dependences. The core idea of quantum computing is to use a small number of qubits to perform computation on the state space of a huge dimension that scales exponentially with the qubit number n. Qubits are therefore the fundamental targets for quantum gates and measurements. Thus to develop a theory to systematically understand quantum circuits we need to focus on how quantum gates affect qubits. Any arbitrary quantum circuit takes in an initial input state, applies a sequence of elementary gates to transform it into a final state, and then measures all or selective qubits in the computational basis. Without loss of generality, we start with the simplest 3-qubit initial state $|000\rangle_{123}$ (where the subscripts 123 denote the qubit number identifiers), then all three qubits start with probability 1 for measuring $|0\rangle$. Now if we apply an arbitrary 1-qubit unitary $U_1(a_1, a_2, \alpha) = \begin{pmatrix} a_1 & a_2^* e^{i\alpha} \\ a_2 & -a_1^* e^{i\alpha} \end{pmatrix}$ (with $|a_1|^2 + |a_2|^2 = 1$) to q_1 then the state becomes $(a_1|0\rangle_1 + a_2|1\rangle_1) \otimes |00\rangle_{23}$ and measuring q_1 will yield the probabilities $p(|0\rangle_1) = |a_1|^2$ and $p(|1\rangle_1) = |a_2|^2$:

Definition 1: The situation that the probabilities of measuring a qubit q_k depend on the parameters of a 1-qubit unitary U_k is defined as "q_k has acquired the dependence on U_k" or alternatively "U_k's dependence has been created on q_k".

By the definition q_1 has acquired the dependence on $U_1(a_1, a_2, \alpha)$ in the above example. Note in this particular example the phase α has no obvious effect on $p(|0\rangle_1)$ or $p(|1\rangle_1)$, but in general it may affect the probabilities in certain cases. Now if we apply another 1-qubit unitary $U_2(b_1, b_2, \beta) = \begin{pmatrix} b_1 & b_2^* e^{i\beta} \\ b_2 & -b_1^* e^{i\beta} \end{pmatrix}$ (with $|b_1|^2 + |b_2|^2 = 1$) to q_2 then the state becomes $(a_1|0\rangle_1 + a_2|1\rangle_1) \otimes (b_1|0\rangle_2 + b_2|1\rangle_2) \otimes |0\rangle_3$, and q_2 has acquired the dependence on $U_2(b_1, b_2, \beta)$. Now if we apply the CNOT gate $CX_{1\to2}$ with the subscript $1 \to 2$ meaning q_1 is the control and q_2 is the target, then the state becomes $[a_1|0\rangle_1 \otimes (b_1|0\rangle_2 + b_2|1\rangle_2) + a_2|1\rangle_1 \otimes (b_2|0\rangle_2 + b_1|1\rangle_2)] \otimes |0\rangle_3$, and now measuring q_2 will yield $p(|0\rangle_2) = |a_1 b_1|^2 + |a_2 b_2|^2$: we see that the probabilities of measuring q_2 now depend on $U_1(a_1, a_2, \alpha)$ too and thus q_2 has acquired the dependence on $U_1(a_1, a_2, \alpha)$ through $CX_{1\to2}$. It is obvious that the control qubit q_1 is unaffected by $CX_{1\to2}$. Next if we apply another CNOT gate $CX_{2\to3}$, then the state becomes $(a_1 b_1|0\rangle_1 + a_2 b_2|1\rangle_1)|00\rangle_{23} + (a_1 b_2|0\rangle_1 + a_2 b_1|1\rangle_1)|11\rangle_{23}$, and measuring q_3 will yield $p(|0\rangle_3) = |a_1 b_1|^2 + |a_2 b_2|^2$ such that q_3 has acquired all the dependences on q_2 – both $U_1(a_1, a_2, \alpha)$ and
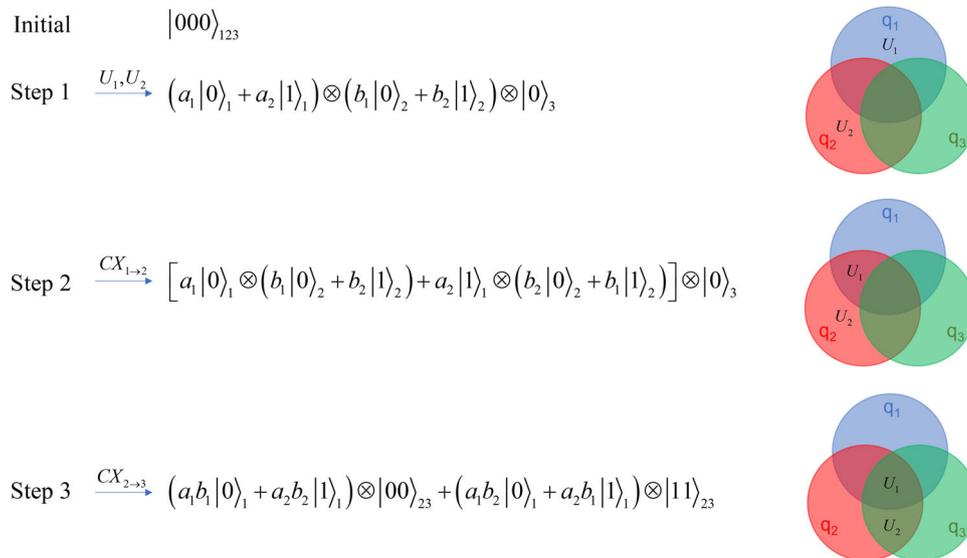
Fig. 1 The creation and copying of unitary dependences. The figure shows the unitary dependence creation by 1-qubit unitaries and copying by CNOT gates. The state at each step is described by a Venn diagram that shows how unitary dependences are shared among the qubits. The unitary dependences are created by the 1-qubit unitaries $U_1 = U_1(a_1, a_2, \alpha) = \begin{pmatrix} a_1 & a_2^* e^{i\alpha} \\ a_2 & -a_1^* e^{i\alpha} \end{pmatrix}$ (with $|a_1|^2 + |a_2|^2 = 1$) and $U_2 = U_2(b_1, b_2, \beta) = \begin{pmatrix} b_1 & b_2^* e^{i\beta} \\ b_2 & -b_1^* e^{i\beta} \end{pmatrix}$ (with $|b_1|^2 + |b_2|^2 = 1$). Then the dependences are copied by the CNOT gates $CX_{1\to2}$ and $CX_{2\to3}$ to the appropriate qubits. At the final Step 3 we have U_2 shared by q_2 and q_3, and U_1 shared by all three qubits.

$U_2(b_1, b_2, \beta)$ – through $CX_{2\to3}$. To summarize the entire process, we started with $|000\rangle_{123}$ having no dependence on any 1-qubit unitary for any qubit, created $U_1(a_1, a_2, \alpha)$'s dependence on q_1, created $U_2(b_1, b_2, \beta)$'s dependence on q_2, copied q_1's dependence to q_2 by $CX_{1\to2}$, and copied q_2's dependences to q_3 by $CX_{2\to3}$.

Figure 1 shows the entire process of dependence creation by 1-qubit unitaries and copying by CNOT gates. At each step, the dependence picture is illustrated by a Venn diagram that clearly shows how the unitary dependences are shared by the qubits. At the final Step 3 we have $U_2(b_1, b_2, \beta)$ shared by q_2 and q_3, and $U_1(a_1, a_2, \alpha)$ shared by all three qubits. The dependence picture clearly tells us that the probabilities of all three qubits are dependent such that they cannot be considered independent random variables when measured. Furthermore, changing the parameters a_1 and a_2 of $U_1(a_1, a_2, \alpha)$ will modify the probabilities of all three qubits, while changing b_1 and b_2 of $U_2(b_1, b_2, \beta)$ will modify only q_2 and q_3. As there is no 1-qubit unitary unique to any qubit, in this circuit we cannot specifically modify a single qubit by changing the parameters of either $U_1(a_1, a_2, \alpha)$ or $U_2(b_1, b_2, \beta)$.

Having seen a simple 3-qubit example, next we propose the rules for a general n-qubit system that:

Rule 1: A 1-qubit unitary U_k applied to the qubit q_k creates its dependence on q_k only;

Rule 2: A CNOT gate $CX_{j\to k}$ copies all the control qubit q_j's dependences to the target qubit q_k.

A special case of Rule 1 has been proven in Theorem 1 of our previous quantum encryption study[35] for real parameters in unitaries and states. Below we generalize the proof to complex parameters:

Proof for Rule 1: An arbitrary n-qubit state can be written as the Schmidt decomposition form with respect to any given q_k:

$$|\phi^{(n)}\rangle = C_1 |\phi_1^{(n-1)}\rangle (a_1 |0\rangle_k + a_2 |1\rangle_k) + C_2 |\phi_2^{(n-1)}\rangle (a_2^* |0\rangle_k - a_1^* |1\rangle_k) e^{i\alpha} \tag{1}$$

where $|\phi_1^{(n-1)}\rangle$ and $|\phi_2^{(n-1)}\rangle$ are orthogonal $(n-1)$-qubit states that exclude q_k, C_1 and C_2 are non-negative real numbers

satisfying $|C_1|^2 + |C_2|^2 = 1$, a_1 and a_2 are complex numbers satisfying $|a_1|^2 + |a_2|^2 = 1$. Clearly the probability of measuring $|0\rangle$ on q_k is $p(|0\rangle_k) = |C_1 a_1|^2 + |C_2 a_2|^2$ and thus we may generalize the definition of unitary dependence to say that q_k has the dependences on the two pairs of coefficients (C_1, C_2) and (a_1, a_2). Both (C_1, C_2) and (a_1, a_2) can include the dependences of many 1-qubit unitaries that were used to create $|\phi^n\rangle$. However, because $|\psi_1\rangle = a_1 |0\rangle_k + a_2 |1\rangle_k$ and $|\psi_2\rangle = (a_2^* |0\rangle_k - a_1^* |1\rangle_k) e^{i\alpha}$ are orthogonal, (a_1, a_2) is a "local dependence" that only applies to q_k while (C_1, C_2) is a "shared dependence" that q_k may share with other qubits. Now if we apply $U_k = \begin{pmatrix} u_1 & u_2^* e^{i\theta} \\ u_2 & -u_1^* e^{i\theta} \end{pmatrix}$ on q_k, as $|U_k \psi_1\rangle$ is always orthogonal to $|U_k \psi_2\rangle$, the dependence on U_k will be added to the local dependence and thus only q_k will acquire it. This proves Rule 1 that a 1-qubit unitary U_k applied to the qubit q_k creates its dependence on q_k only.

Proof for Rule 2: The action of a CNOT gate $CX_{j\to k}$ is to keep q_k intact when $q_j = |0\rangle$ and bit-flip q_k if $q_j = |1\rangle$ – this effectively calculates the binary sum $q_k \oplus q_j$ and stores its value on q_k[26,36–39]. When we measure q_k after $CX_{j\to k}$, the probabilities of getting $|0\rangle$ and $|1\rangle$ are actually the probabilities of getting $q_k \oplus q_j = 0$ and $q_k \oplus q_j = 1$, thus all the 1-qubit unitaries that affect q_j's measurement probabilities will now also affect q_k's probabilities after $CX_{j\to k}$. In the meanwhile, it is obvious that q_j's measurement probabilities are not affected by $CX_{j\to k}$. Therefore Rule 2 has been proven that "A CNOT gate $CX_{j\to k}$ copies all the control qubit q_j's dependences to the target qubit q_k".

The unitary dependence theory allows us to generate dependence pictures as illustrated by the Venn diagrams in Fig. 1. The dependence picture of a quantum circuit or state provides two important pieces of information that characterize its behaviors. The first piece is how the measurement probabilities of qubits depend on each other in the output state. If multiple qubits share dependences on a certain collection of 1-qubit unitaries, their measurement results will behave as dependent

random variables; if multiple qubits do not share any unitary dependences, their measurement results will behave as independent random variables. The dependence picture thus allows us to characterize the measurement statistics of the output state, which is an important property of a quantum circuit or state[9]. The second piece is how the qubits can be manipulated together by varying parameters of the shared 1-qubit unitaries. If a 1-qubit unitary is shared by multiple qubits, varying its parameters can change the measurement probabilities of all involved qubits together, thus allowing collective manipulations of subgroups of qubits. On the other hand, if the manipulation of an individual qubit is needed, then the qubit must have 1-qubit unitaries not shared by any other qubits. This is a design principle that can guide the development of e.g., parameterized quantum circuits[18,27,40,41] where circuits and ansatz states are tested by varying gate parameters.

Advantages over the entanglement description of quantum circuits and states. The unitary dependence theory and the dependence picture are distinct from the conventional way of using entanglement to understand quantum circuits and states. In this section we detail the differences between the two theories and show the advantages of the dependence picture over the entanglement description.

Entanglement is an important subject in quantum physics that demonstrates quantum-only features that have no classical equivalent. However, from the perspective of quantum circuit design, entanglement is too abstract and not easily connected to the practicalities discussed above on how qubits are related in manipulations and measurement probabilities. To see this, consider the state:

$$|\psi\rangle = (a_1|00\rangle_{12} + a_2|11\rangle_{12}) \otimes b_1|0\rangle_3 + (a_1|01\rangle_{12} + a_2|10\rangle_{12}) \otimes b_2|1\rangle_3 \quad (2)$$

where a_1, a_2, b_1, b_2 are complex numbers satisfying $|a_1|^2 + |a_2|^2 = 1$ and $|b_1|^2 + |b_2|^2 = 1$. In $|\psi\rangle$, q_1 and q_3 are considered entangled because there is no separable way to write the two qubits as a product state. However, by simple inspection we have $p(|0\rangle_1) = |a_1|^2$ and $p(|0\rangle_3) = |b_1|^2$ – i.e., q_1 only has dependence on the pair (a_1, a_2) while q_3 only has dependence on the pair (b_1, b_2) – which means q_1 and q_3 have independent measurement probabilities and can be manipulated separately. So the entanglement picture fails to characterize the relation between q_1 and q_3. In the meanwhile, by the unitary dependence theory, $|\psi\rangle$ is created by the process shown in Fig. 2 and the relation between q_1 and q_3 can be easily seen in the Venn diagram.

In Fig. 2, we have $U_1(a_1, a_2, \alpha)$ shared by q_1 and q_2, and $U_3(b_1, b_2, \beta)$ shared by q_2 and q_3, therefore q_1 and q_3 share no 1-qubit unitaries and are independent for both measurement and manipulation. This example clearly shows the dependence picture is fundamentally different from the entanglement picture because two entangled qubits may have no shared dependence and thus are considered to be independent by the dependence theory.

Using entanglement to describe quantum circuits and states can become more confusing when considering multiple-qubit systems where many different measures and theories for multipartite entanglement exist[28–30]. For example, for a 3-qubit system there are the Greenberger–Horne–Zeilinger (GHZ) state $|GHZ\rangle = \frac{1}{\sqrt{2}}(|000\rangle + |111\rangle)$ and the W state $|W\rangle = \frac{1}{\sqrt{3}}(|001\rangle + |010\rangle + |100\rangle)$, which are well-known to be different and can be explained by various multipartite entanglement measures[28–30]. However, most multipartite entanglement measures generate some numbers for fixed values of parameters and thus cannot characterize parameterized quantum circuits and states: e.g., $a_1|000\rangle + a_2|111\rangle$ will produce different values of the

von Neumann entropy, given different values for a_1 and a_2. In the meanwhile the dependence picture is naturally suited to the ideas of using finite structures with varying parameters to characterize large collections of quantum circuits and states together:[26,42] e.g., $a_1|000\rangle + a_2|111\rangle$ can be described by one simple Venn diagram in Fig. 3.

Although there is a theory to generalize the GHZ state and W state into the GHZ class and W class[29], the process of determining the class for an arbitrary state involves calculating the determinants of all the possible bipartite reduced density matrices and then the 3-tangle:[28,29] this is a very complex process and more importantly not describing the qubit relation in measurement and manipulation. For example, it is not obvious whether the state $|\psi\rangle$ in Eq. (2) belongs to the GHZ or W class, and even if we can determine its class, it has a dependence picture (see Fig. 2) distinct from both the GHZ and W classes in Figs. 3 and 4 such that the entanglement class does not describe the qubit relation of interest in the current study. On the other hand the dependence pictures in Figs. 2, 3, and 4 clearly show the differences between the three states by illustrating the relation of qubits in manipulation and measurement. Furthermore, when the number of qubits increases beyond 3, the number of possible entanglement classes becomes infinite and there is no practical way to determine the class for an arbitrary state[29]. On the other hand, no matter how many qubits there are, the dependence picture can always be easily generated by going through the gate sequence associated with any quantum circuit or state, one gate at a time. So as long as the gate count is polynomial the process of determining the dependence picture is polynomial. When the number of qubits increases it may be difficult to draw the Venn diagram, but the dependence picture can still be easily described by listing the qubits with the unitary dependences they have, and listing the 1-qubit unitaries with the qubits they belong to. For example, the W state dependence picture in Fig. 4 can be alternatively described by

The W state unitary dependence description

by qubits $\quad (q_1 : \{R_y(\theta_1), X\}, q_2 : \{R_y(\theta_1), R_y(\theta_2), R_y(\theta_3)\},$
$\qquad q_3 : \{R_y(\theta_1), R_y(\theta_2), R_y(\theta_3)\})$

by 1 − qubit unitaries $\quad (R_y(\theta_1) : \{q_1, q_2, q_3\}, R_y(\theta_2) : \{q_2, q_3\}, X : \{q_1\},$
$\qquad R_y(\theta_3) : \{q_2, q_3\})$

$$(3)$$

and this description always works for systems with more qubits.

When studying the behavior of quantum circuits and states involving many qubits, there are often cases where we want to temporarily focus on a subset of qubits and treat the other qubits as an averaging background. For entanglement, the qubits that are considered entangled in the total system may become unentangled in the subsystem. For example, the GHZ-like entangled state $a_1|000\rangle + a_2|111\rangle$ will become the reduced density matrix $\rho = a_1|00\rangle\langle00| + a_2|11\rangle\langle11|$ when any one of the qubits is removed, and this is clearly an unentangled (separable) mixed state[43]. This shows that entanglement is sensitive to how we partition the space into subsets of qubits. On the other hand, the dependence picture is robust regardless how we partition the space as we can take the Venn diagrams or the descriptions like in Eq. (3), remove all the unwanted qubits, and the remaining parts will describe the correct relations among the qubits of interest. Again using the example of $a_1|000\rangle + a_2|111\rangle$ shown in Fig. 3, removing any one of the qubits will remove one circle from the Venn diagram, which does not change the relation between the two remaining circles: sharing U_1, therefore the relation between the two remaining qubits stays the same in the absence of the removed qubit. This illustrates the fact that the dependences of qubits on 1-qubit unitaries are more robust physical properties
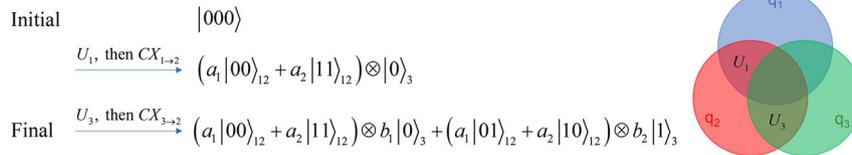
Fig. 2 The case of entangled qubits not sharing any unitary dependence. The figure shows the creation process of $|\psi\rangle$ and the final unitary dependence picture represented by a Venn diagram. $U_1 = U_1(a_1, a_2, \alpha) = \begin{pmatrix} a_1 & a_2^* e^{i\alpha} \\ a_2 & -a_1^* e^{i\alpha} \end{pmatrix}$ (with $|a_1|^2 + |a_2|^2 = 1$) and $U_3 = U_3(b_1, b_2, \beta) = \begin{pmatrix} b_1 & b_2^* e^{i\beta} \\ b_2 & -b_1^* e^{i\beta} \end{pmatrix}$ (with $|b_1|^2 + |b_2|^2 = 1$) are 1-qubit unitaries applied to q_1 and q_3 respectively. From the final unitary dependence picture we see q_1 and q_3 do not share any 1-qubit unitaries and thus are independent in measurement probabilities. However q_1 and q_3 are entangled, thus the unitary dependence picture provides a different perspective from the entanglement description.

that are invariant upon partitioning of the system, while the concept of entanglement is less robust that may change upon partitioning of the system.

The dependence canceling rule and the application to analyzing the hardware-efficient ansatzes. Having seen the basic rules of dependence creation and copying in the "Basic rules for the creation and copying of unitary dependences" subsection in the "Results and Discussion", next we discuss the situation where dependences originated from the same unitary source can cancel when duplicated on the same qubit. In the simplest case, $CX_{1\rightarrow 2}$ copies all dependences of q_1 to q_2, and another $CX_{1\rightarrow 2}$ will attempt to copy all the same dependences again from q_1 to q_2. As $CX_{1\rightarrow 2}$ is its own inverse, the 2nd $CX_{1\rightarrow 2}$ thus cancels all dependences copied by the 1st $CX_{1\rightarrow 2}$. A more interesting case happens when the dependence originated from the same unitary source is received from different qubits. For example, consider the 3-qubit state:

$$(a_1|0\rangle_1 + a_2|1\rangle_1) \otimes (b_1|0\rangle_2 + b_2|1\rangle_2) \otimes (c_1|0\rangle_3 + c_2|1\rangle_3) \quad (4)$$

which starts with q_1 depending on (a_1, a_2), q_2 depending on (b_1, b_2), q_3 depending on (c_1, c_2). Now if we apply $CX_{2\rightarrow 1}$ and $CX_{2\rightarrow 3}$, it becomes:

$$(a_1|0\rangle_1 + a_2|1\rangle_1) \otimes b_1|0\rangle_2 \otimes (c_1|0\rangle_3 + c_2|1\rangle_3) + (a_2|0\rangle_1 + a_1|1\rangle_1) \otimes b_2|1\rangle_2 \otimes (c_2|0\rangle_3 + c_1|1\rangle_3) \quad (5)$$

where q_1 and q_3 have both acquired dependence on (b_1, b_2). Now if we apply $CX_{1\rightarrow 3}$, then the state becomes:

$$|0\rangle_1 \otimes [a_1 b_1 |0\rangle_2 \otimes (c_1|0\rangle_3 + c_2|1\rangle_3) + a_2 b_2 |1\rangle_2 \otimes (c_2|0\rangle_3 + c_1|1\rangle_3)]$$
$$+ |1\rangle_1 \otimes [a_2 b_1 |0\rangle_2 \otimes (c_2|0\rangle_3 + c_1|1\rangle_3) + a_1 b_2 |1\rangle_2 \otimes (c_1|0\rangle_3 + c_2|1\rangle_3)] \quad (6)$$

where q_3 has lost the dependence on (b_1, b_2) because after some algebra we find that $p(|0\rangle_3) = |a_1 c_1|^2 + |a_2 c_2|^2$. Here the effect of $CX_{1\rightarrow 3}$ is attempting to copy both (a_1, a_2) and (b_1, b_2) dependences from q_1 to q_3, however because q_3 has already received (b_1, b_2) from q_2, receiving the same dependence again from q_1 will duplicate and cancel it on q_3. Here we propose the general canceling rule of unitary dependences.

Definition 2: Multiple dependences are considered "the same" if they are copied from the same qubit q_i by some CNOT gates and there are no 1-qubit unitaries in between these CNOT gates. Furthermore, these dependences stay the same no matter how many times they are copied by more CNOT gates and which qubits they are on, as long as there are no 1-qubit unitaries applied.

Rule 3: If a qubit q_k receives the same dependence twice, it will lose (cancel) that dependence.

Proof for Rule 3: As discussed in the proof for Rule 2, $CX_{i\rightarrow j}$ calculates the binary sum $q_i \oplus q_j$ and stores its value on q_j, and if

we next apply e.g., $CX_{j\rightarrow k}$ then it calculates the binary sum $q_i \oplus q_j \oplus q_k$ and stores its value on q_k. Note as long as there are no 1-qubit unitaries and only CNOTs, we can continue to perform such binary additions with more CNOT gates, so as to update the current "configuration" represented by an account of the current value held by each qubit. This process can be clearly described by the "qubit functional configuration" (QFC) where we start with the initial QFC (for details of the QFC theory please see the original study[26]):

$$(f_1 = q_1, f_2 = q_2, f_3 = q_3 ..., f_n = q_n) \quad (7)$$

for which each f_k (i.e., the qubit functional on q_k) represents the current value stored on the corresponding qubit q_k. Now if we apply e.g., $CX_{1\rightarrow 2}$, we update f_2 to be $f_2 = q_1 \oplus q_2$ with other f_k intact so the QFC becomes:

$$(f_1 = q_1, f_2 = q_1 \oplus q_2, f_3 = q_3 ..., f_n = q_n) \quad (8)$$

Now if we apply another CNOT gate e.g., $CX_{2\rightarrow 3}$, we update f_3 to be $f_3 = q_1 \oplus q_2 \oplus q_3$ and the QFC becomes:

$$(f_1 = q_1, f_2 = q_1 \oplus q_2, f_3 = q_1 \oplus q_2 \oplus q_3 ..., f_n = q_n) \quad (9)$$

where we see that although q_1 has not directly interacted with q_3, it has nonetheless been connected to q_3 by the two CNOT gates and the connection is clear from the QFC where f_1 and f_3 share the same component of q_1. Here we notice the interesting fact that, the connection of f_1 and f_3 sharing the same component of q_1 also means q_1 and q_3 sharing the dependences that already exist on q_1 before the $CX_{1\rightarrow 2}$ gate. This is clear because by Rule 2 above, $CX_{1\rightarrow 2}$ copies all dependence from q_1 to q_2, and then $CX_{2\rightarrow 3}$ copies all dependence from q_2 to q_3 – we see that the process of the qubit functionals getting updated by some CNOT gates is essentially the same as the process of the unitary dependences getting copied by the same CNOT gates. In other words, take Eq. (9) as an example, $f_2 = q_1 \oplus q_2$ means q_2 shares the dependences initially on q_1, while $f_3 = q_1 \oplus q_2 \oplus q_3$ means q_3 shares the dependences initially on q_1 and q_2. With the equivalence between the two processes understood, it becomes clear why duplicated dependences get canceled: no matter from which qubit q_k receives the 1st copy of q_i's initial dependences, its corresponding functional f_k now has q_i as a component, and then the attempt to add a 2nd copy of q_i's initial dependences will add q_i to f_k again, and this cancels q_i on f_k because $q_i \oplus q_i = 0$. In addition, it also becomes clear why the canceling requires the condition of no 1-qubit unitaries, because only then can we stay in the same QFC addition process or as described in the original QFC study[26] "in the same QFC layer", while any 1-qubit unitary will require the QFC getting reset to the initial configuration. In terms of the unitary dependence theory, if q_k receives the 1st copy of q_i's dependences from q_j after a 1-qubit unitary U_j on q_j, the dependences could be modified by U_j such that they are no
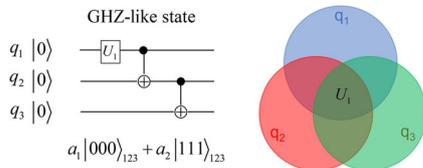
Fig. 3 The dependence picture of the GHZ-like state. The figure shows the creation circuit of the GHZ-like state and the Venn diagram of the unitary dependence picture. $U_1 = U_1(a_1, a_2, \alpha) = \begin{pmatrix} a_1 & a_2^* e^{i\alpha} \\ a_2 & -a_1^* e^{i\alpha} \end{pmatrix}$ is a 1-qubit unitary applied to q_1. When the parameters satisfy $a_1 = a_2 = \frac{1}{\sqrt{2}}$ the state becomes the GHZ state.
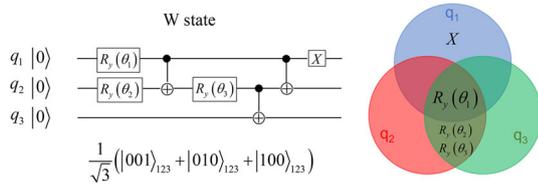

Fig. 4 The dependence picture of the W state. The figure shows the creation circuit of the W state and the Venn diagram of the dependence picture. The gates and the parameters are defined as:

$R_y(\theta) = \begin{pmatrix} \cos\frac{\theta}{2} & -\sin\frac{\theta}{2} \\ \sin\frac{\theta}{2} & \cos\frac{\theta}{2} \end{pmatrix}$, $\theta_1 = 2\arccos(\frac{1}{\sqrt{3}})$, $\theta_2 = -\theta_3 = \frac{\pi}{4}$.
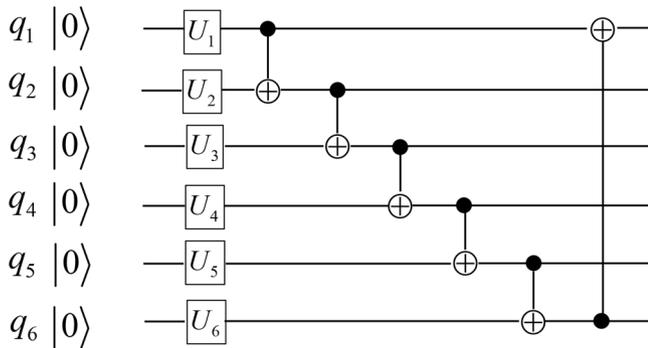

Fig. 5 The 1st example of the hardware-efficient ansatz. The figure shows the quantum circuit of one layer of the hardware-efficient ansatz in ref. [33] U_1 through U_6 are 1-qubit unitaries applied to the qubits q_1 through q_6, respectively. The CNOT gate layer then copies the unitary dependencies around the qubits. The final unitary dependence picture as described in Eq. (10) shows the qubits are highly-dependent on manipulations and measurement statistics.

longer the same as the initial ones. Now when q_k receives the 2nd copy from q_h before any 1-qubit unitary U_h on q_h, then this copy stays the same as the initial one, thus the two copies of dependences are not the same and may not cancel. This concludes the proof for Rule 3.

The QFC description of quantum circuits and states not only helps us prove Rule 3, but can also be useful for identifying connections between qubits with no apparent interactions. In Definition 2 we have the fact that "dependences stay the same no matter how many times they are copied by more CNOT gates and which qubits they are on, as long as there are no 1-qubit unitaries applied". This means two qubits may acquire the same dependences without ever interacting directly and they will be dependent when manipulated or measured. In addition, canceling
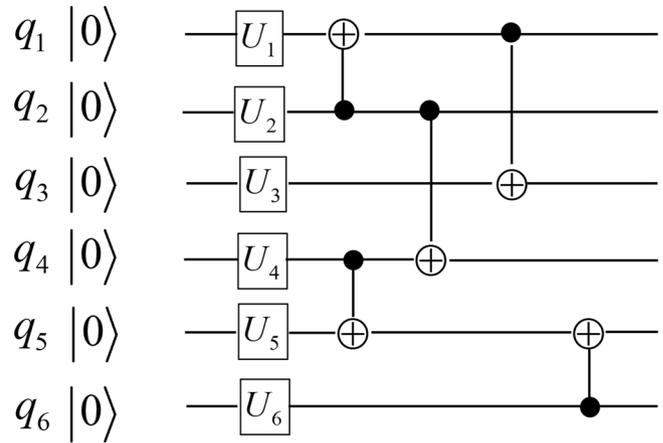

Fig. 6 The 2nd example of the hardware-efficient ansatz. The figure shows the quantum circuit of one layer of the hardware-efficient ansatz in ref. [34] U_1 through U_6 are 1-qubit unitaries applied to the qubits q_1 through q_6, respectively. The CNOT gate layer then copies the unitary dependencies around the qubits. The final unitary dependence picture as described in Eq. (11) shows the qubits are more independent in manipulations and measurement statistics.

of those dependences will happen when sometime later the two qubits directly interact with a CNOT gate.

To illustrate the application of all three rules working together to obtain the complete unitary dependence picture, here we consider the hardware-efficient ansatz that is widely used in variational quantum algorithms[31–34]. The main feature of the hardware-efficient ansatz is that each ansatz layer includes two sub-layers: one sub-layer of parameterized 1-qubit unitaries and one sub-layer of two-qubit entanglers. When the two-qubit entanglers are all CNOT gates, there is no 1-qubit unitary in between the entanglers and the entangler sub-layer can be considered as a single layer of the qubit functional configuration (QFC) as described above—this means the canceling rule works perfectly within one entangler sub-layer and we can easily obtain the unitary dependence picture of each ansatz layer. In two examples, the ansatzes used in the original studies[33,34] are shown in Figs. 5 and 6, respectively, and the unitary dependence pictures (in Eq. (3)'s description form of the picture) are shown in Eqs. (10) and (11), respectively.

The unitary dependence picture of the ansatz in ref. [33].

$$
\begin{aligned}
&(q_1 : \{U_2 \sim U_6\}, q_2 : \{U_1, U_2\}, q_3 : \{U_1 \sim U_3\}, q_4 : \{U_1 \sim U_4\}, \\
&q_5 : \{U_1 \sim U_5\}, q_6 : \{U_1 \sim U_6\}) \\
&(U_1 : \{q_2 \sim q_6\}, U_2 : \{q_1 \sim q_6\}, U_3 : \{q_1, q_3 \sim q_6\}, U_4 : \{q_1, q_4 \sim q_6\}, \\
&U_5 : \{q_1, q_5, q_6\}, U_6 : \{q_1, q_6\})
\end{aligned}
\tag{10}
$$

The unitary dependence picture of the ansatz in ref. [34]:

$$
\begin{aligned}
&(q_1 : \{U_1, U_2\}, q_2 : \{U_2\}, q_3 : \{U_1 \sim U_3\}, q_4 : \{U_2, U_4\}, q_5 : \{U_4 \sim U_6\}, q_6 : \{U_6\}) \\
&(U_1 : \{q_1, q_3\}, U_2 : \{q_1 \sim q_4\}, U_3 : \{q_3\}, U_4 : \{q_4, q_5\}, U_5 : \{q_5\}, U_6 : \{q_5, q_6\})
\end{aligned}
\tag{11}
$$

Here the unitary dependence pictures of both ansatzes are generated by following the quantum gates one by one while considering Rules 1 to 3 to determine what each gate does to the evolving unitary dependence picture. A basic example of this process can be found in Fig. 1 where the Venn diagram is generated by three steps (with the two 1-qubit unitaries combined into one step). For the current example of the ansatz in Fig. 5, by Rule 1 the six 1-qubit unitaries create one dependence on each qubit; then by Rule 2 $CX_{1\to 2}$ copies U_1 to q_2, $CX_{2\to 3}$ copies U_1 and U_2 to q_3, and so on ...; then by Rules 2 and 3, $CX_{6\to 1}$ copies

all unitaries to q_1 and U_1 is canceled—the final result is the unitary dependence picture in Eq. (10). This example shows the process of generating the unitary dependence picture is directly related to the process of building the ansatz itself, so the complexity of generating the unitary dependence picture is the same as the complexity of the ansatz, which in the current case of "hardware-efficient ansatzes" is linear in the qubit number.

Now what useful information is provided by the unitary dependence pictures of these ansatzes? Firstly, the unitary dependence pictures provide both intuitive and precise descriptions of the unitary dependences assigned to each qubit: we can see exactly which qubits depend on which unitaries. Some information available from the unitary dependence picture may not be obvious by inspecting the circuit alone: one example is the fact of q_1 not depending on U_1 in Fig. 5, which can be deduced by applying Rules 2 and 3: U_1 has been copied to q_6 by a series of CNOT gates and then canceled on q_1 by $CX_{6\rightarrow1}$; another example is the fact of q_3 depending on U_2 in Fig. 6, which can be deduced by applying Rule 2: U_2 has been copied to q_1 by $CX_{2\rightarrow1}$, and then to q_3 by $CX_{1\rightarrow3}$. The precise description of exactly which qubits depend on which unitaries makes the unitary dependence theory advantageous over existing descriptions such as the "causal cone" approach[44–46] that only identifies rough correlations between subgroups of qubits and quantum gates.

Secondly, the unitary dependence pictures show the practical connections among the qubits in manipulations and measurement statistics, which are also not obvious by inspecting the circuits alone. For example, inspecting the circuits in Fig. 5 and Fig. 6, we can say in either ansatz all the qubits are entangled to each other, but the difference between the two ansatzes is not obvious. However, the top line of the unitary dependence picture in Eq. (11) clearly shows that q_2 only depends on U_2 and q_6 only depends on U_6, which means the measurement statistics of these two qubits are independent from other qubits. Additionally on the bottom line in Eq. (11), U_3 only affects q_3 and U_5 only affects q_5, which means these two qubits can be individually manipulated without modifying other qubits. On the other hand, in the unitary dependence picture in Eq. (10) the qubits are more connected in the sense that all qubits depend on multiple unitaries and all unitaries affect multiple qubits. Therefore by the unitary dependence pictures we immediately know that the measurement and manipulation of the qubits are more connected in Fig. 5 and more disconnected in Fig. 6 —thus the two ansatzes can behave very differently during a variational process when the parameters of the unitaries are optimized.

Using the useful information provided by the unitary dependence pictures, next we propose an idea for a systematic study to improve the performances of ansatzes. Suppose we are using a variational quantum algorithm[31–34] to find the minimum of an optimization problem: e.g., the ground energy of a molecular Hamiltonian. The two ansatzes in Figs. 5 and 6 are likely to have different convergence rates or even converge to different values if the iteration numbers are limited—these can be used to evaluate the performances of the ansatzes. Now if for a particular problem the ansatz in Fig. 5 does better, it may imply the problem prefers the ansatz to have more connected qubits, or vice versa. We can then add more CNOT gates to increase the connectivity or remove some CNOT gates to reduce the connectivity and see if the performance improves or worsens. This way we may be able to systematically find better ansatzes and understand why some ansatzes perform badly for a particular problem. Going through the same process for a variety of problems, we may even see the problems themselves separate into one group that prefers disconnected ansatzes and the other that prefers connected ansatzes – thus the ansatz properties described

by the unitary dependence pictures may be used to characterize not only the ansatzes, but also the problems.

Note if two copies of dependences are not considered the same by Definition 2, they may or may not cancel when copied to the same qubit. Consider the simple example of a 2-qubit state:

$$|\phi\rangle = (a_1|0\rangle_1 + a_2|1\rangle_1) \otimes (b_1|0\rangle_2 + b_2|1\rangle_2) \quad (12)$$

with q_1 depending on (a_1, a_2) and q_2 depending on (b_1, b_2). Now applying $CX_{1\rightarrow2}$ we have:

$$|CX_{1\rightarrow2}\phi\rangle = a_1|0\rangle_1 \otimes (b_1|0\rangle_2 + b_2|1\rangle_2) + a_2|1\rangle_1 \otimes (b_2|0\rangle_2 + b_1|1\rangle_2) \quad (13)$$

and by Rule 2, q_2 now depends on both (b_1, b_2) and (a_1, a_2) with $p(|0\rangle_2) = |a_1b_1|^2 + |a_2b_2|^2$. By Rule 3, if we apply $CX_{1\rightarrow2}$ again then (a_1, a_2) will be canceled from q_2, but if we apply a 1-qubit unitary $U_2 = \begin{pmatrix} u_1 & u_2^* \\ u_2 & -u_1^* \end{pmatrix}$ on q_2 first, then $CX_{1\rightarrow2}$, we have:

$$|CX_{1\rightarrow2} \cdot U_2 \cdot CX_{1\rightarrow2}\phi\rangle = a_1|0\rangle_1 \otimes [(u_1b_1 + u_2^*b_2)|0\rangle_2 + (u_2b_1 - u_1^*b_2)|1\rangle_2]$$
$$+ a_2|1\rangle_1 \otimes [(u_2b_2 - u_1^*b_1)|0\rangle_2 + (u_1b_2 + u_2^*b_1)|1\rangle_2] \quad (14)$$

and the probability of measuring $|0\rangle$ for q_2 is:

$$p(|0\rangle_2) = |a_1|^2|u_1b_1 + u_2^*b_2|^2 + |a_2|^2|u_2b_2 - u_1^*b_1|^2 \quad (15)$$

which still has dependence on (a_1, a_2), i.e., canceling did not happen. This is clearly due to U_2's modification of the 1st copy of (a_1, a_2) received by q_2.

However, a more intriguing scenario happens if we entangle a 3rd qubit $q_3 = |0\rangle_3$ to q_2 by applying $CX_{2\rightarrow3}$ to the state $|CX_{1\rightarrow2}\phi\rangle$ as in Eq. (13), we have:

$$|CX_{2\rightarrow3} \cdot CX_{1\rightarrow2}\phi\rangle = a_1|0\rangle_1 \otimes (b_1|00\rangle_{23} + b_2|11\rangle_{23}) + a_2|1\rangle_1 \otimes (b_2|00\rangle_{23} + b_1|11\rangle_{23}) \quad (16)$$

where by Rule 2 we have copied q_2's dependences to, while there is no apparent change to q_1 and q_2. If we now apply $U_2 = \begin{pmatrix} u_1 & u_2^* \\ u_2 & -u_1^* \end{pmatrix}$ on q_2 and then $CX_{1\rightarrow2}$, we have:

$$|CX_{1\rightarrow2} \cdot U_2 \cdot CX_{2\rightarrow3} \cdot CX_{1\rightarrow2}\phi\rangle$$
$$= a_1|0\rangle_1 \otimes [b_1(u_1|0\rangle_2 + u_2|1\rangle_2) \otimes |0\rangle_3 + b_2(u_2^*|0\rangle_2 - u_1^*|1\rangle_2) \otimes |1\rangle_3]$$
$$+ a_2|1\rangle_1 \otimes [b_2(u_2|0\rangle_2 + u_1|1\rangle_2) \otimes |0\rangle_3 + b_1(-u_1^*|0\rangle_2 + u_2^*|1\rangle_2) \otimes |1\rangle_3] \quad (17)$$

and the probability of measuring $|0\rangle$ for q_2 is:

$$p(|0\rangle_2) = |a_1|^2(|u_1b_1|^2 + |u_2^*b_2|^2) + |a_2|^2(|u_2b_2|^2 + |u_1^*b_1|^2)$$
$$= |u_1b_1|^2 + |u_2b_2|^2 \quad (18)$$

which has no dependence on (a_1, a_2). So although Rule 3's condition is violated by U_2 before the 2nd $CX_{1\rightarrow2}$, canceling still happens! By comparing Eq. (13) with (16), (14), with (17), we see the only difference between the two is, in the 2nd case, q_2 is entangled to q_3 before U_2, and this suggests that entanglement can protect the cancellability from getting broken by local 1-qubit unitaries. To understand this interesting phenomenon, we observe the state in Eq. (13) q_1 and q_2 are entangled, such that a local unitary U_2 on q_2 may affect the dependence on (a_1, a_2) that is shared by the two qubits. On the other hand, if we trace out q_3 in Eq. (16) to get the reduced density matrix of q_1 and q_2,

we have:

$$Tr_3(\rho) = Tr_3(|CX_{2\to3} \cdot CX_{1\to2}\phi\rangle\langle CX_{2\to3} \cdot CX_{1\to2}\phi|)$$
$$= (|a_1b_1|^2 + |a_2b_2|^2)|\varphi_1\rangle\langle\varphi_1| + (|a_1b_2|^2 + |a_2b_1|^2)|\varphi_2\rangle\langle\varphi_2|$$
$$|\varphi_1\rangle = \frac{(a_1b_1|0\rangle_1 + a_2b_2|1\rangle_1)}{\sqrt{|a_1b_1|^2+|a_2b_2|^2}} \otimes |0\rangle_2 \qquad |\varphi_2\rangle = \frac{(a_1b_2|0\rangle_1 + a_2b_1|1\rangle_1)}{\sqrt{|a_1b_2|^2+|a_2b_1|^2}} \otimes |1\rangle_2$$

(19)

where the reduced density matrix of q_1 and q_2 is a mixture of two pure product states $|\varphi_1\rangle$ and $|\varphi_2\rangle$, and the shared dependence on (a_1, a_2) only affects q_2 through the pure state probabilities $p_1 = |a_1b_1|^2 + |a_2b_2|^2$ and $p_2 = |a_1b_2|^2 + |a_2b_1|^2$. Clearly, any 1-qubit unitaries on q_2 will only affect the qubit locally and will not affect the pure state probabilities, and this is the reason why canceling holds even after U_2. The effect of entanglement is to break the entangled state in Eq. (13) into product states in the 2-qubit reduced system in Eq. (19), and this causes the canceling of dependences to happen even when local 1-qubit unitaries are applied to q_2. This example may suggest a mechanism for using entanglement with additional qubits to protect certain properties of the system against local disturbances.

Conclusions

In this work, we develop a unitary dependence theory to characterize the behaviors of quantum circuits and states in terms of how 1-qubit unitaries and CNOT gates affect qubits and determine their measurement probabilities. In particular, we define the basic rules of dependence creation by 1-qubit unitaries and copying by CNOT gates: 1. a 1-qubit unitary U_k makes the qubit q_k's measurement probabilities depend on U_k; 2. a CNOT gate $CX_{j\to k}$ copies all the control qubit q_j's dependences to the target qubit q_k. By these rules, after a gate sequence of a quantum circuit, the final state can be described by a complete dependence picture that shows which qubits depend on which 1-qubit unitaries. The dependence picture carries important information of whether the measurement results of qubits are dependent or independent, and whether multiple qubits can be manipulated together or separately. Compared to the abstract formalism of multi-qubit entanglement, the dependence picture is more directly connected to the practicalities of using parameterized quantum gates to manipulate qubits and create desirable measurement statistics in the output states. In addition, the dependence picture is easier to use for many-qubit systems and more robust upon system partitioning. Under certain conditions, the dependences originated from the same unitary source can cancel when duplicated on the same qubit, which reduces complexity and simplifies the dependence picture. A particularly interesting case arises when studying the cancellability of dependences is that entanglement with an additional qubit may protect the cancellability from getting broken by local 1-qubit unitaries. This may suggest a mechanism for using entanglement with additional qubits to protect certain properties of the system against local disturbances. Finally, the theory has been applied to the widely-used hardware-efficient ansatz to demonstrate its ability to characterize the behaviors of different ansatzes in variational quantum algorithms.

Data availability

Data sharing is not applicable to this article as no datasets were generated or analyzed during the current study.

References
1. Smart, S. E., Hu, Z., Kais, S. & Mazziotti, D. A. Relaxation of stationary states on a quantum computer yields a unique spectroscopic fingerprint of the computer's noise. *Commun. Phys.* **5**, 28 (2022).
2. Georgescu, I. M., Ashhab, S. & Nori, F. Quantum simulation. *Rev. Mod. Phys.* **86**, 153–185 (2014).
3. Montanaro, A. Quantum algorithms: an overview. *npj Quantum Inform.* **2**, 15023 (2016).
4. Cao, Y. et al. Quantum chemistry in the age of quantum computing. *Chem. Rev.* **119**, 10856–10915 (2019).
5. Albash, T. & Lidar, D. A. Adiabatic quantum computation. *Rev. Mod. Phys.* **90**, 015002 (2018).
6. Preskill, J. Quantum computing in the NISQ era and beyond. *Quantum* **2**, 79 (2018).
7. Kais, S. ed. Quantum Information and Computation for Chemistry. (John Wiley & Sons; 2014).
8. Preskill, J. Quantum computing 40 years later. arXiv:2106.10522 [quant-ph], (2021).
9. Arute, F. et al. Quantum supremacy using a programmable superconducting processor. *Nature* **574**, 505–510 (2019).
10. Boixo, S. et al. Evidence for quantum annealing with more than one hundred qubits. *Nat. Phys.* **10**, 218–224 (2014).
11. Linke, N. M. et al. Experimental comparison of two quantum computing architectures. *Proc. Natl Acad. Sci.* **114**, 3305 (2017).
12. Carolan, J. et al. Universal linear optics. *Science* **349**, 711 (2015).
13. Zhong, H.-S. et al. Quantum computational advantage using photons. *Science* **370**, 1460 (2020).
14. Gong, M. et al. Quantum walks on a programmable two-dimensional 62-qubit superconducting processor. *Science* **372**, 948 (2021).
15. Kitaev, A. Y. Quantum computations: algorithms and error correction. *Russ. Math. Surv.* **52**, 1191 (1997).
16. Shor, P. W. Polynomial-time algorithms for prime factorization and discrete logarithms on a quantum computer. *SIAM J. Comput.* **26**, 1484–1509 (1997).
17. Harrow, A. W., Hassidim, A. & Lloyd, S. Quantum algorithm for linear systems of equations. *Phys. Rev. Lett.* **103**, 150502 (2009).
18. Peruzzo, A. et al. A variational eigenvalue solver on a photonic quantum processor. *Nat. Commun.* **5**, 4213 (2014).
19. Daskin, A. & Kais, S. Decomposition of unitary matrices for finding quantum circuits: application to molecular Hamiltonians. *J. Chem. Phys.* **134**, 144112 (2011).
20. Biamonte, J. et al. Quantum machine learning. *Nature* **549**, 195–202 (2017).
21. Xia, R. & Kais, S. Quantum machine learning for electronic structure calculations. *Nat. Commun.* **9**, 4195 (2018).
22. Sajjan, M., Sureshbabu, S. H. & Kais, S. Quantum machine-learning for eigenstate filtration in two-dimensional materials. *J. Am. Chem. Soc.* **143**, 18426–18445 (2021).
23. Hu, Z., Xia, R. & Kais, S. A quantum algorithm for evolving open quantum dynamics on quantum computing devices. *Sci. Rep.* **10**, 3301 (2020).
24. Wang, H., Ashhab, S. & Nori, F. Quantum algorithm for simulating the dynamics of an open quantum system. *Phys. Rev. A* **83**, 062317 (2011).
25. Hu, Z. et al. A general quantum algorithm for open quantum dynamics demonstrated with the Fenna-Matthews-Olson complex dynamics. *Quantum* **6**, 726 (2022).
26. Hu, Z. & Kais S. Characterizing quantum circuits with qubit functional configurations. *Sci. Rep.* **13**, 5539 (2023).
27. Sim, S., Johnson, P. D. & Aspuru-Guzik, A. Expressibility and entangling capability of parameterized quantum circuits for hybrid quantum-classical algorithms. *Adv. Quantum Technol.* **2**, 1900070 (2019).
28. Coffman, V., Kundu, J. & Wootters, W. K. Distributed entanglement. *Phys. Rev. A* **61**, 052306 (2000).
29. Dür, W., Vidal, G. & Cirac, J. I. Three qubits can be entangled in two inequivalent ways. *Phys. Rev. A* **62**, 062314 (2000).
30. Huber, M. & de Vicente, J. I. Structure of multidimensional entanglement in multipartite systems. *Phys. Rev. Lett.* **110**, 030501 (2013).
31. Tilly, J. et al. The Variational Quantum Eigensolver: a review of methods and best practices. *Physics Reports* **986**, 1–128 (2021).
32. Cerezo, M. et al. Variational quantum algorithms. *Nat. Rev. Phys.* **3**, 625–644 (2021).
33. Wang, Y., Li, G. & Wang, X. Variational quantum gibbs state preparation with a truncated Taylor series. *Phys. Rev. Appl.* **16**, 054035 (2021).
34. Kandala, A. et al. Hardware-efficient variational quantum eigensolver for small molecules and quantum magnets. *Nature* **549**, 242–246 (2017).
35. Hu, Z. & Kais, S. A quantum encryption design featuring confusion, diffusion, and mode of operation. *Sci. Rep.* **11**, 23774 (2021).
36. Hu, Z. & Kais, S. The quantum condition space. *Adv. Quantum Technol.* **5**, 2100158 (2022).

37. Amy, M., Maslov, D. & Mosca, M. Polynomial-time T-depth optimization of clifford+T circuits via matroid partitioning. *IEEE Trans. Comput.-Aided Des. Integr. Circuits Syst.* **33**, 1476–1489 (2014).

38. Amy, M., Azimzadeh, P. & Mosca, M. On the controlled-NOT complexity of controlled-NOT–phase circuits. *Quantum Sci. Technol.* **4**, 015002 (2018).

39. Hu, Z. & Kais S. The wave-particle duality of the qudit quantum space and the quantum wave gates. arXiv:2207.05213, (2022).

40. Farhi, E., Goldstone J. & Gutmann S. A quantum approximate optimization algorithm. arXiv:1411.4028 [quant-ph], (2014).

41. Benedetti, M. et al. Parameterized quantum circuits as machine learning models. *Quantum Sci. Technol.* **4**, 043001 (2019).

42. Hu, Z. & Kais S. Characterization of quantum states based on creation complexity. *Adv. Quantum Technol.* **3**, 2000043 (2020).

43. Peres, A. Separability criterion for density matrices. *Phys. Rev. Lett.* **77**, 1413–1415 (1996).

44. Benedetti, M., Fiorentini, M. & Lubasch, M. Hardware-efficient variational quantum algorithms for time evolution. *Phys. Rev. Res.* **3**, 033083 (2021).

45. Uvarov, A. V. & Biamonte, J. D. On barren plateaus and cost function locality in variational quantum algorithms. *J. Phys. A Math. Theor.* **54**, 245301 (2021).

46. Anand, A. et al. Information flow in parameterized quantum circuits. arXiv:2207.05149 (2022).

Acknowledgements

Author contributions

S.K. and Z.H. conceived the project. S.K. supervised the project. Z.H. developed the theory and performed the analysis. Z.H. and S.K. wrote and reviewed the manuscript.

Competing interests

The authors declare no competing interests.

Additional information

Correspondence and requests for materials should be addressed to Sabre Kais.

Peer review information *Communications Physics* thanks Jules Tilly, Takeshi Sato, and the other, anonymous, reviewer(s) for their contribution to the peer review of this work.

Reprints and permission information is available at http://www.nature.com/reprints

Publisher's note Springer Nature remains neutral with regard to jurisdictional claims in published maps and institutional affiliations.